Electronic Supplementary Information

Leucine zipper motif inspiration: a two-dimensional Leucine Velcro-like array in peptide coordination polymers generates hydrophobicity

Sabina Rodríguez-Hermida,[a] Emi Evangelio,[a] Marta Rubio-Martínez,[a] Inhar Imaz,[a] Albert Verdaguer,[a] Jordi Juanhuix,[b] and Daniel Maspoch*[a,c]

[a] Catalan Institute of Nanoscience and Nanotechnology (ICN2), CSIC and The Barcelona Institute of Science and Technology, Campus UAB, Bellaterra, 08193 Barcelona, Spain.

[b] Alba Synchrotron Light Facility, 08290 Cerdanyola del Vallés, Barcelona, Spain.

[c] ICREA, Pg. Lluís Companys 23, 08010 Barcelona, Spain.

* Corresponding author, E-mail: daniel.maspoch@icn2.cat

S1. Experimental Section

S1.1. Materials

All chemical reagents and solvents were purchased from commercial sources and used as received without further purification. $Zn(NO_3)_2 \cdot 6H_2O$ and $Zn(CH_3COO)_2 \cdot 2H_2O$ were purchased from Sigma Aldrich. Asp-Leu was purchased from GenScript, whereas Leu-Asp·HCl and Asp-Leu-Leu were purchased from SynPeptide.

S1.2. Characterization

FTIR. All spectra were recorded on a Bruker Tensor 27FTIR equipped with a Golden Gate diamond ATR cell.

Elemental analysis. All analyses were collected on a CHNS Thermo Scientific Flash 2000 elemental analyzer.

Thermogravimetric analysis. TGA were performed under N_2 (20 $mLmin^{-1}$ flow rate), on a Perkin Elmer Pyris 1 (heating rate: 10 ^oC/min; temperature range: 25 ^oC to 600 ^oC).

Powder X-ray Diffraction. PXRD was recorded at room temperature on an X'Pert PRO MPD diffractometer (PanAnalytical) for Cu Kα radiation (λ = 1.5418 Å).

SEM. Field-Emission Scanning Electron Microscopy (FESEM) images were collected on a FEI Quanta 650F scanning electron microscope at an acceleration voltage of 20.0 KV, using aluminium as support. Samples were metallized with Pt.

Formation of the pressed disk pellets. Twenty mg of sample were ground to a fine powder that was subsequently pressed under 2 tons of pressure for 5 minutes to provide a 5-mm-diameter disk.

Contact angle measurements. For pressed-pellet disks, static and dynamic (receding and advancing) contact angle measurements were performed on a Krüss DSA 100 drop shape analyzer. A 5-μL droplet of deionized water was placed onto the sample surface in sessile mode at a speed of 135.2 $\mu Lmin^{-1}$. For hand-packed powders, the static contact angle measurements were collected on a Krüss EasyDrop analyzer using an 8-μL water droplet.

Surface roughness measurements. Atomic Force Microscopy (AFM) images of the surfaces were obtained under ambient conditions (T = 22 ^oC, RH ~ 40%) using amplitude modulation AFM (AM-AFM) mode with a MFP3D AFM (Asylum Research, Santa Barbara). Non-contact silicon cantilevers (PPP-FM, Nanosensors) were employed, with a resonant frequency of $f_0 \approx 70$ kHz and a spring constant of $k \approx 4$ Nm^{-1}. Roughness ratio (r) was calculated from a 25 x 25 μm image by taking the ratio between the textured surface area of the image and its cross-sectional area (625 μm^2) using the Gwyddion software. The values reported of r are averages from five different images taken at different spots of the sample that were separated by at least 1 mm of space.

S1.3. Crystallography

Crystallographic data for **1-3** were collected at 100 K at the XALOC beamline at the ALBA synchrotron[1] (λ = 0.82656 Å for **1**, λ = 0.82653 Å for **2**, and λ = 0.89843 Å for **3**). Plate faces were indexed for crystal 1 by taking six 0.5° oscillation images equally spaced 45° apart. Appropriate scattering factors were applied using XDISP.[2] Data were indexed, integrated and scaled using the XDS program. Absorption corrections were not applied. The structures were solved by direct methods and subsequently refined by correction of F^2 against all reflections, using SHELXS2013 and SHELXL2013 within the WinGX package.[3-5] All non-hydrogen atoms were refined with anisotropic thermal parameters by full-matrix least-squares calculations on F^2. Hydrogen atoms were refined as riders, except for the hydrogen atoms of the –NH and –NH_2 groups in **2**, which were located based on the difference Fourier map. In **3**, the hydrogen atoms of the coordinated water molecule were not possible to be localized on the difference Fourier map. The best single crystal of **3** was investigated, but it was still weakly diffracting (as the all several measured crystals); therefore, EADP, DELU and SIMU constraint and restraints were applied in order to correctly model the crystal structure. In **1**, high residual density peak was found near the metal center and therefore, Zn(II) ion was refined over two positions with 90% and 10% occupancy. The structural data have been deposited at the Cambridge Crystallographic Data Centre (CCDC) under reference numbers 1507367, 1507368 and 1507369 for **1**, **2** and **3**, respectively (Tables S1-S5).

Table S1. Crystal and structural refinement data for **1-3.**

Compound	**1**	**2**	**3**
Empirical formula	$C_{10}H_{16}N_2O_5Zn$	$C_{10}H_{16}N_2O_5Zn$	$C_{16}H_{29}N_3O_7Zn$
Formula weight	309.62	309.62	440.79
Crystal system	Monoclinic	Orthorhombic	Monoclinic
Space group	$P2_1$	$P2_12_12_1$	$P2_1$
CCDC reference	1507367	1507368	1507369
Unit cell dimensions			
a (Å)	5.440(4)	7.590(3)	8.700(5)
b (Å)	6.0700(10)	11.390(2)	6.200(5)
c (Å)	19.8000(10)	13.990(10)	18.520(4)
β (°)	94.836(11)	90	98.090(5)
V ($Å^3$)	651.5(5)	1209.4(10)	989.0(10)
Z	2	4	2
F(000)	320	640	460
θ range (°)	2.401 – 33.693	2.682 – 33.730	1.404 - 33.926
Indep. ref. (R_{int})	2548 (0.055)	2771 (0.0585)	3136 (0.386)
Final R indices [I>2sigma(I)]	R1 = 0.0721 wR2 = 0.1966	R1 = 0.0409 wR2 = 0.1082	R1 = 0.1483 wR2 = 0.3049
Absolute structure parameter	0.030(17)	0.080(6)	0.04(7)

S1.4. Synthesis of 1

A solution of $Zn(NO_3)_2.6H_2O$ (6 mg, 0.02 mmol) in a mixture of 2 mL of water and 1 mL of EtOH was added to a solution containing Asp-Leu (5 mg, 0.02 mmol) in 3 mL of MilliQ water (pH of the peptide solution adjusted to 9 with NaOH). The resulting solution was heated at 85 °C for 24 hours. Colorless plate crystals of **1** were filtered off, washed with water and vacuum-dried. Yield: 0.010 g (25%). Anal. found: C, 38.84; H, 5.19; N, 8.88; $ZnC_{10}H_{16}N_2O_5$ requires: C, 38.79; H, 5.21; N, 9.05. FTIR: ν (cm^{-1}) = 3225m + 3136w + 3073w + 2957m (CH, NH, NH_2), 1655m (C=O), 1578s (OCO_{asym}), 1390s (OCO_{sym}).

S1.5. Synthesis of 2

A solution of $Zn(CH_3COO)_2{\cdot}2H_2O$ (10 mg; 0.04 mmol) in 1 mL of EtOH was added to an aqueous solution containing Leu-Asp (10 mg; 0.04 mmol) in 1 mL of MilliQ water. The resulting solution was heated at 85 °C for 24 hours. Colorless prism crystals of **2** filtered off, washed with water and vacuum-dried. Yield: 0.009 g (25%). Anal. found: C, 38.00; H, 5.36; N, 8.50; $ZnC_{10}H_{16}N_2O_5$ requires: C, 38.79; H, 5.21; N, 9.05. FTIR: ν (cm^{-1}) = 3233m + 3160m + 3051m + 2949m (CH, NH, NH2), 1624s (C=O), 1550s (OCO_{asym}), 1366s (OCO_{sym})

S1.6. Synthesis of 3

A solution of $Zn(NO_3)_2.6H_2O$ (11.4 mg, 0.04 mmol) in 5 mL of MilliQ water was added to a basic solution containing Asp-Leu-Leu (30 mg, 0.08 mmol) in 5 mL of MilliQ water (pH of the peptide solution adjusted to 10 with NaOH). The resulting solution was heated at 85 °C for 48 hours. Colorless needle crystals of **3** were filtered off, washed with water and ethanol, and vacuum-dried. Yield: 0.010 g (27%). Anal. found: C, 43.56; H, 6.64; N, 9.25; $ZnC_{16}H_{27}N_3O_7$ requires: C, 43.80; H, 6.20; N, 9.58. FTIR: ν (cm^{-1}) = 3298m + 3113w + 2947w + 2864m (CH, NH, NH_2), 1652m (C=O), 1606m (OCO_{asym}), 1365m (OCO_{sym}).

Table S2. Selected bond distances (Å) and angles (°) for **1**.[a] Bond distances and angles corresponding to the metal center with 90% of occupancy (Zn(1a)) are only shown.

		O(2)$^{\#1}$-Zn(1a)-O(4)	173.6(3)
		O(4)-Zn(1a)-N(1)$^{\#1}$	98.7(3)
		O(3)$^{\#2}$-Zn(1a)-O(4)	88.0(3)
Zn(1a)-O(4)	2.046(8)	O(1)$^{\#3}$-Zn(1a)-O(4)	90.2(3)
Zn(1a)-O(2)$^{\#1}$	2.213(7)	O(2)$^{\#1}$-Zn(1a)-N(1)$^{\#1}$	87.5(3)
Zn(1a)-N(1)$^{\#1}$	2.017(7)	O(2)$^{\#1}$-Zn(1a)-O(3)$^{\#2}$	92.7(3)
Zn(1a)-O(3)$^{\#2}$	2.039(7)	O(1)$^{\#3}$-Zn(1a)-O(2)$^{\#1}$	83.5(3)
Zn(1a)-O(1)$^{\#3}$	1.937(7)	O(3)$^{\#2}$-Zn(1a)-N(1)$^{\#1}$	99.7(3)
		O(1)$^{\#3}$-Zn(1a)-N(1)$^{\#1}$	151.7(3)
		O(1)$^{\#3}$-Zn(1a)-O(3)$^{\#2}$	107.5(3)

[a] Symmetry transformations used to generate equivalent atoms: #1 -1+x,-1+y,z; #2 x,-1+y,z; #2 2-x,-1/2+y,1-z.

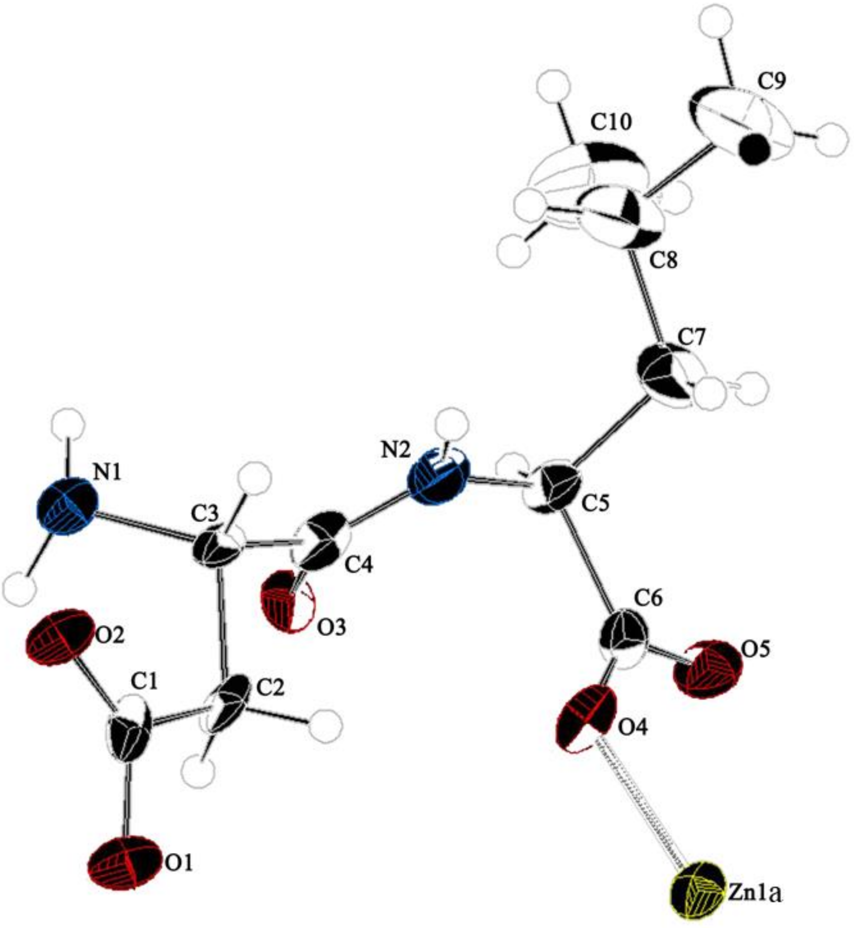

Table S3. Selected bond distances (Å) and angles (°) for **2**.[a]

		O(1)$^{\#1}$-Zn(1)-O(2)$^{\#1}$	60.86(13)
		O(1)$^{\#1}$-Zn(1)-O(4)$^{\#2}$	94.89(13)
		O(1)$^{\#1}$-Zn(1)-O(5)	86.35(12)
Zn(1)-O(1)$^{\#1}$	2.185(3)	O(1)$^{\#1}$-Zn(1)-N(2)	155.21(14)
Zn(1)-O(2)$^{\#1}$	2.110(3)	O(2)$^{\#1}$-Zn(1)-O(4)$^{\#2}$	113.69(16)
Zn(1)-O(4)$^{\#2}$	1.961(3)	O(2)$^{\#1}$-Zn(1)-O(5)	117.94(14)
Zn(1)-O(5)	2.043(3)	O(2)$^{\#1}$-Zn(2)-N(2)	105.60(15)
Zn(1)-N(2)	2.060(4)	O(4)$^{\#1}$-Zn(2)-O(5)	120.74(15)
		O(4)$^{\#1}$-Zn(2)-N(2)	109.85(15)
		O(5)-Zn(2)-N(2)	82.49(14)

[a] Symmetry transformations used to generate equivalent atoms: #1 5/2-x, 1-y, -1/2+z; #2 3/2-x, 1-y, -1/2+z

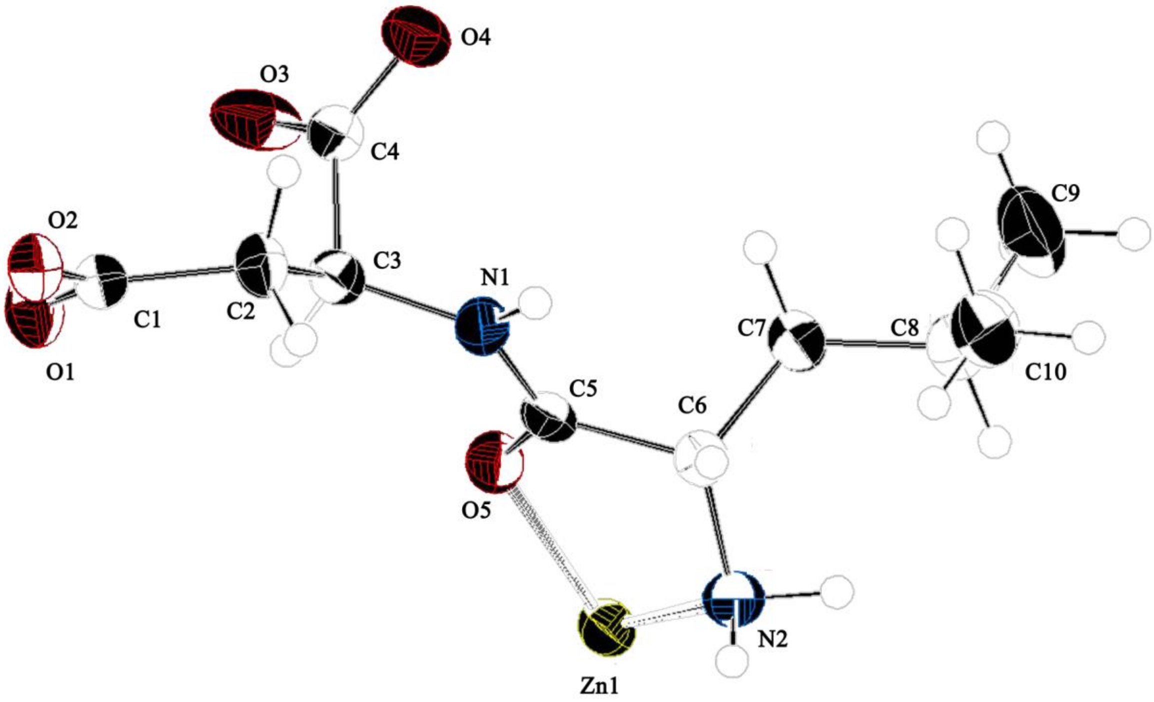

Table S4. Selected bond distances (Å) and angles (°) for **3**.[a]

		O(1w)-Zn(1)-O(3)	174.5(8)
		O(1w)-Zn(1)-N(1)	95.9(11)
		O(1w)-Zn(1)-O(6)$^{\#1}$	92.3(9)
Zn(1)-O(1w)	2.128(19)	O(1w)-Zn(1)-O(2)$^{\#2}$	88.1(9)
Zn(1)-O(3)	2.20(3)	O(3)-Zn(1)-N(1)	80.7(13)
Zn(1)-N(1)	1.97(3)	O(3)-Zn(1)-O(6)$^{\#1}$	93.1(10)
Zn(1)-O(6)$^{\#1}$	1.99(2)	O(3)-Zn(2)-O(2)$^{\#2}$	90.2(10)
Zn(1)-O(2)$^{\#2}$	1.89(2)	O(2)$^{\#2}$-Zn(2)-N(1)	125.0(11)
		O(2)$^{\#2}$-Zn(2)-O(6)$^{\#1}$	102.9(10)
		O(6)$^{\#1}$-Zn(2)-N(1)	131.5(11)

[a] Symmetry transformations used to generate equivalent atoms: #1 -1+x,y,z; #2 x,-1+y,z.

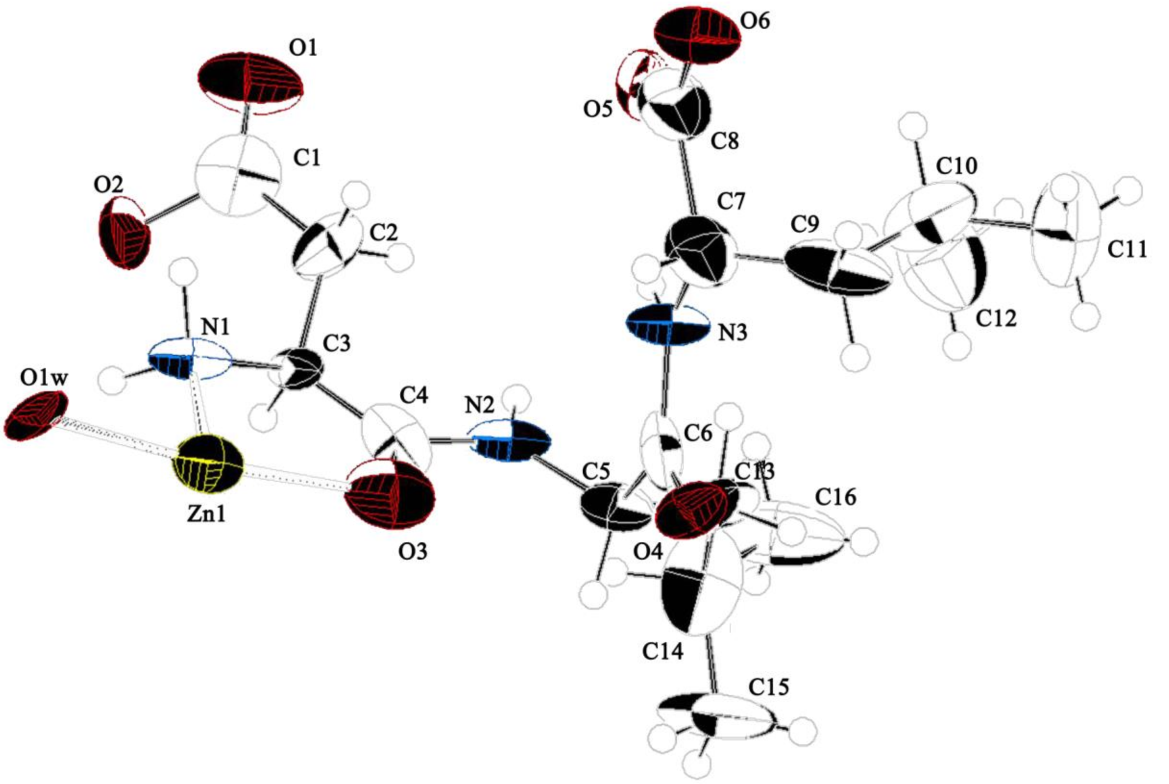

Table S5. H-bond interactions (Å/°) in **1**, **2** and **3**.[a]

D-H…A	**d (D-H)**	**d (H…A)**	**d (D..A)**	**< (DHA)**
Compound ***1***				
N(1)-H(1a)…O(1)$^{\#1}$	0.99	1.96	2.907(9)	160.0
N(1)-H(1b)…O(5)$^{\#2}$	0.99	2.09	2.917(10)	140.3
N(2)-H(2)…O(5)$^{\#3}$	0.88	2.02	2.836(11)	153.0
Compound ***2***				
N(2)-H(2c)…O(3)$^{\#4}$	0.793(19)	2.12(2)	2.908(6)	172(5)
N(1)-H(1a)…O(1)$^{\#5}$	0.83(3)	1.97(3)	2.771(5)	164(6)
Compound ***3***				
N(1)-H(1a)…O(1w)$^{\#6}$	0.99	2.09	2.99(4)	151.7
N(1)-H(1b)…O(1)$^{\#7}$	0.99	1.89	2.87(4)	175.9
N(2)-H(2n)…O(4)$^{\#8}$	0.88	2.19	3.07(3)	170.7
O(1w)…O(5)$^{\#7}$			2.65(3)	
O(1w)…O(6)$^{\#9}$			2.66(3)	

[a] Symmetry transformations used to generate equivalent atoms: #1 -x+2,y+1/2,-z+1; #2 x+1,y+1,z; #3 x+1,y,z; #4 -x+2,y+1/2,-z+3/2; #5 x-1/2,-y+3/2,-z+2; #6 –x+2,y+1/2,-z+1; #7 –x+3,y-1/2,-z+1; #8 x,y+1,z; #9 3-x,y+1/2,1-z.

Figure S1. FTIR spectra of (a) **1** (black) and Asp-Leu (blue), (b) **2** (black) and Leu-Asp (blue), and (c) **3** (black) and Asp-Leu-Leu (blue).

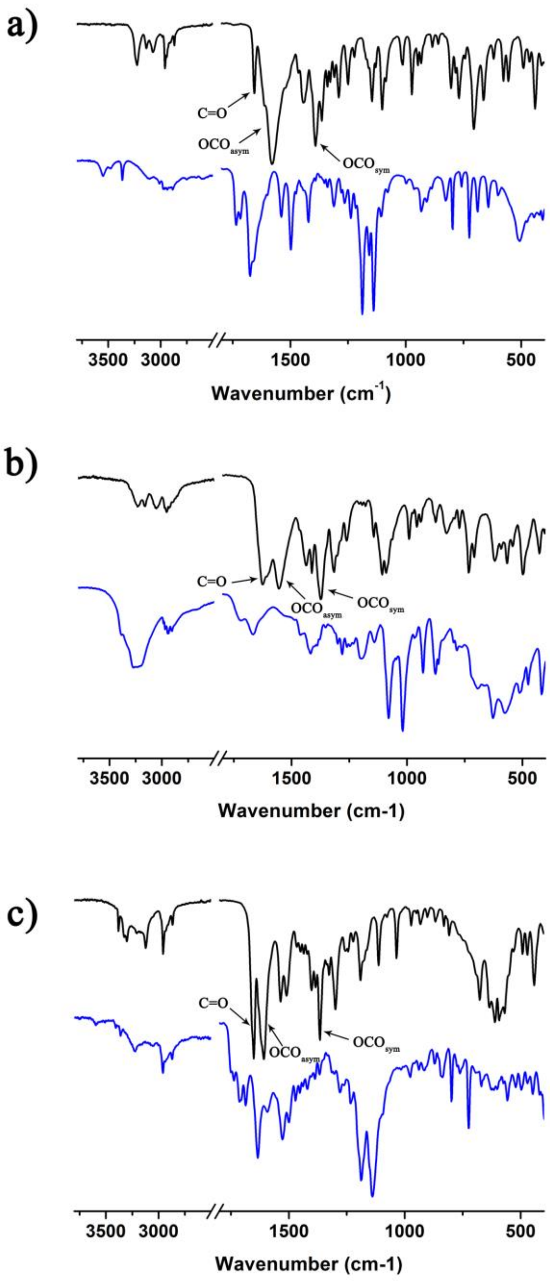

	Stretching bands (cm^{-1})		
	C=O	**OCO$_{asym}$**	**OCO$_{sym}$**
Asp-Leu	1735	1674	1421
1	1655	1578	1390
Leu-Asp	1724	1675	1421
2	1624	1550	1366
Asp-Leu-Leu	1712	1638	1523
3	1652	1606	1365

The IR spectra comparison of **1**, **2** and **3** with their corresponding peptide show the shift of the bands attributed to the carboxylate and amide groups to lower frequencies respect to the free peptides. This shift evidences their coordination to Zn(II) ions

Figure S2. TGA diagrams of **1** (a), **2** (b), and **3** (c).

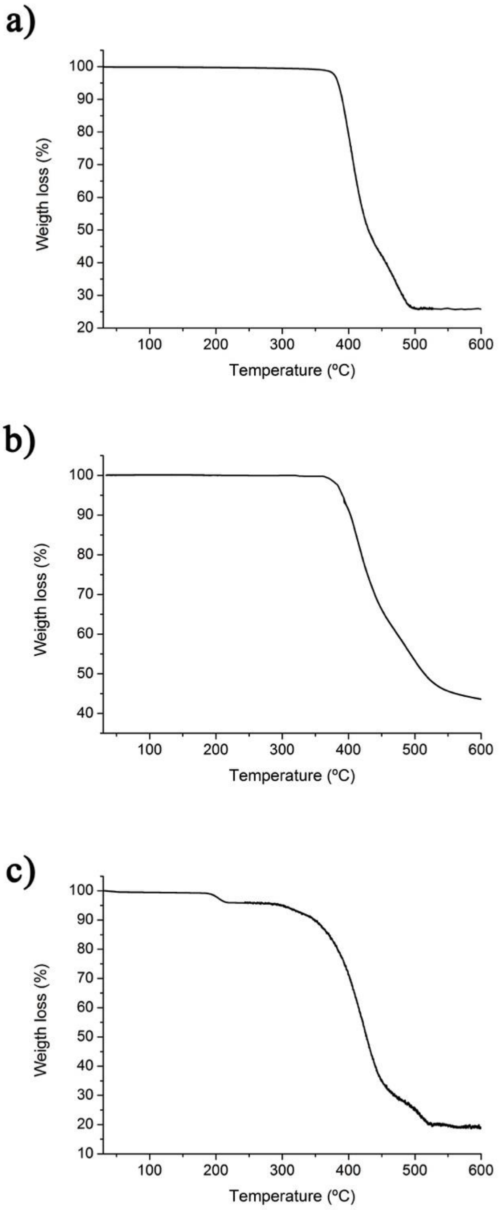

TGA diagrams of **1** and **2** show no weight loss from r.t. to 350 °C, at which point the framework begins to decompose. The TGA profile of **3** reveals an initial weight-loss of 3.36% from 170 °C to 225 °C, attributable to loss of the coordinated water molecule (calc.: 4.12%), and a second weight loss at *ca.* 300 °C, at which point the structure begins to decompose.

Figure S3. For **1**, the experimental PXRD pattern (red) and the simulated pattern from its crystal structure (black).

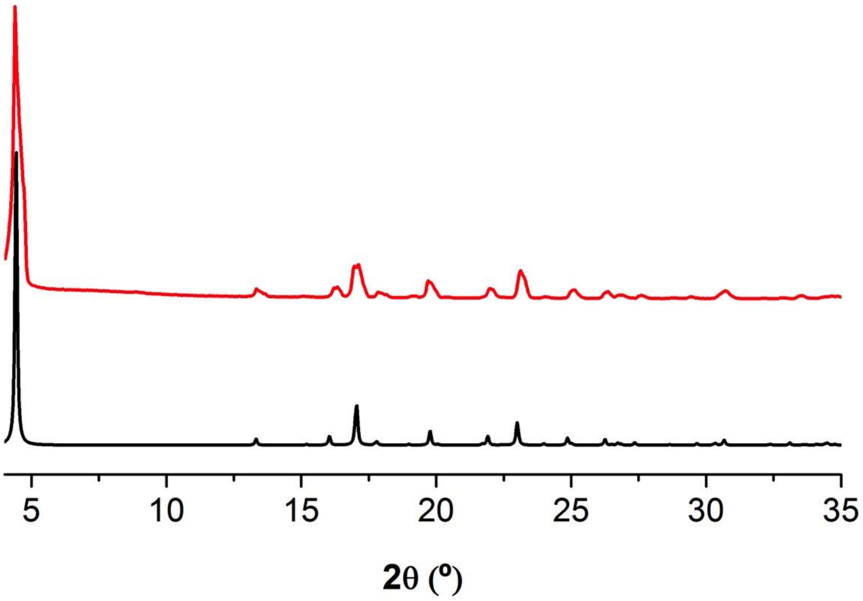

Figure S4. For **2**, the experimental PXRD pattern (red) and the simulated pattern from its crystal structure (black).

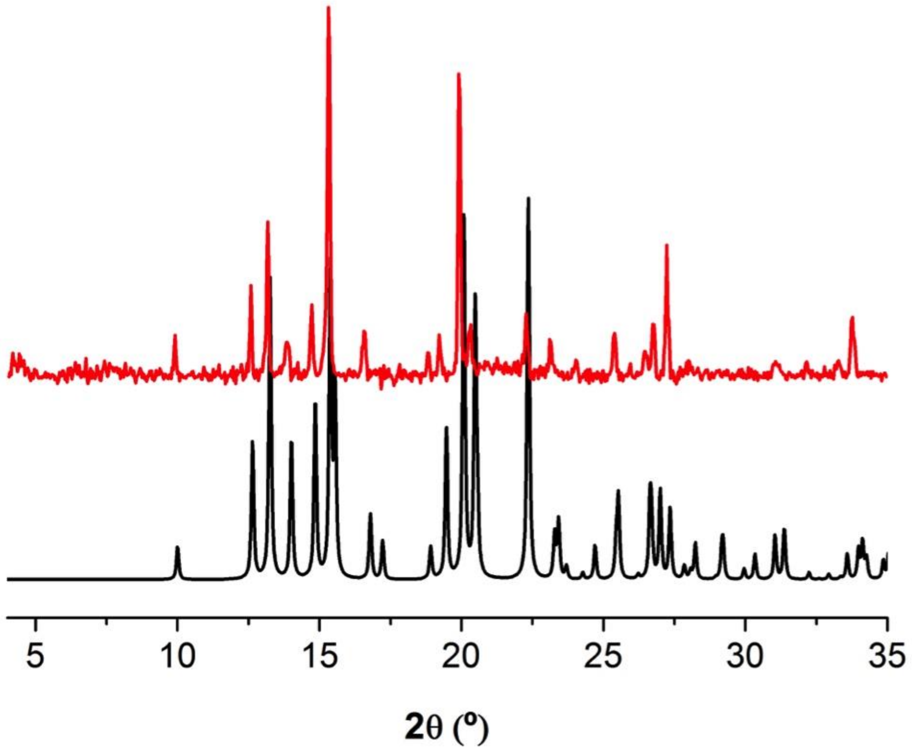

Figure S5. For **3**, the experimental PXRD pattern (red) and the simulated pattern from its crystal structure (black).

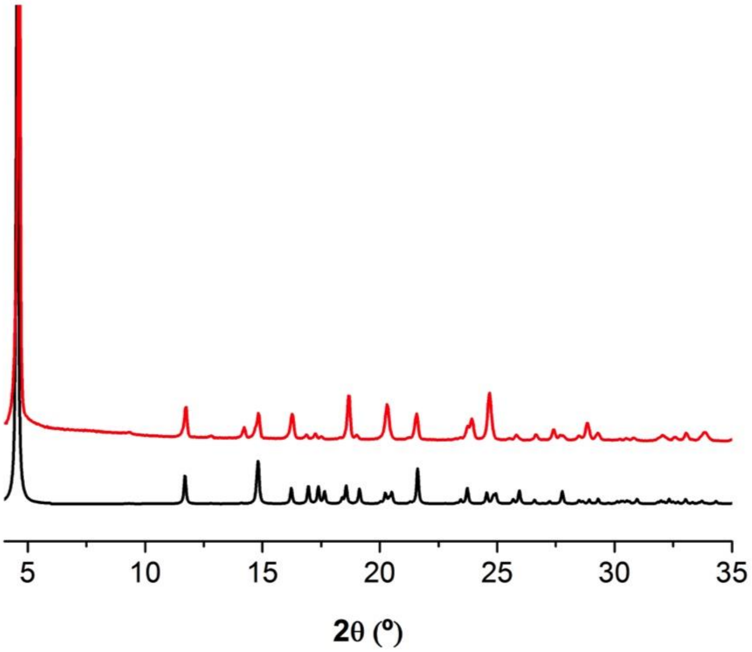

Figure S6. SEM images of **1** (a), **2** (b), and **3** (c). The scale bars correspond to 100 μm (a), 200 μm (b), and 50 μm (c).

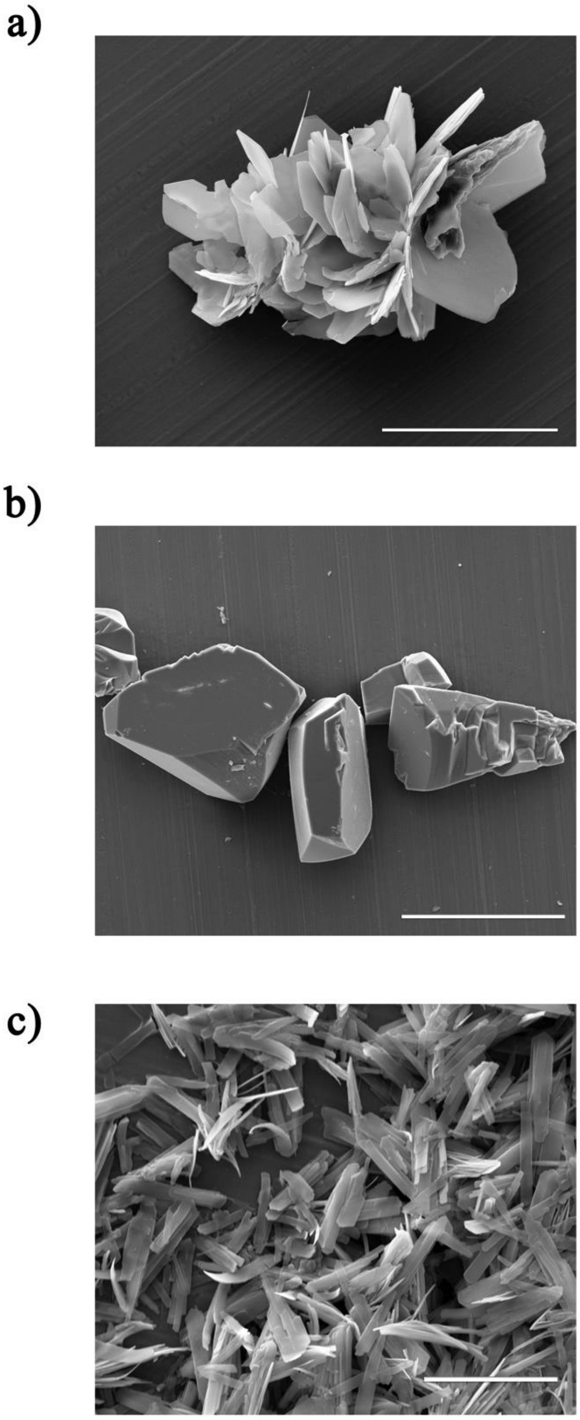

Figure S7. The coordination environment surrounding the Zn(II) ions in **1** (a), **2** (b), and **3** (c).

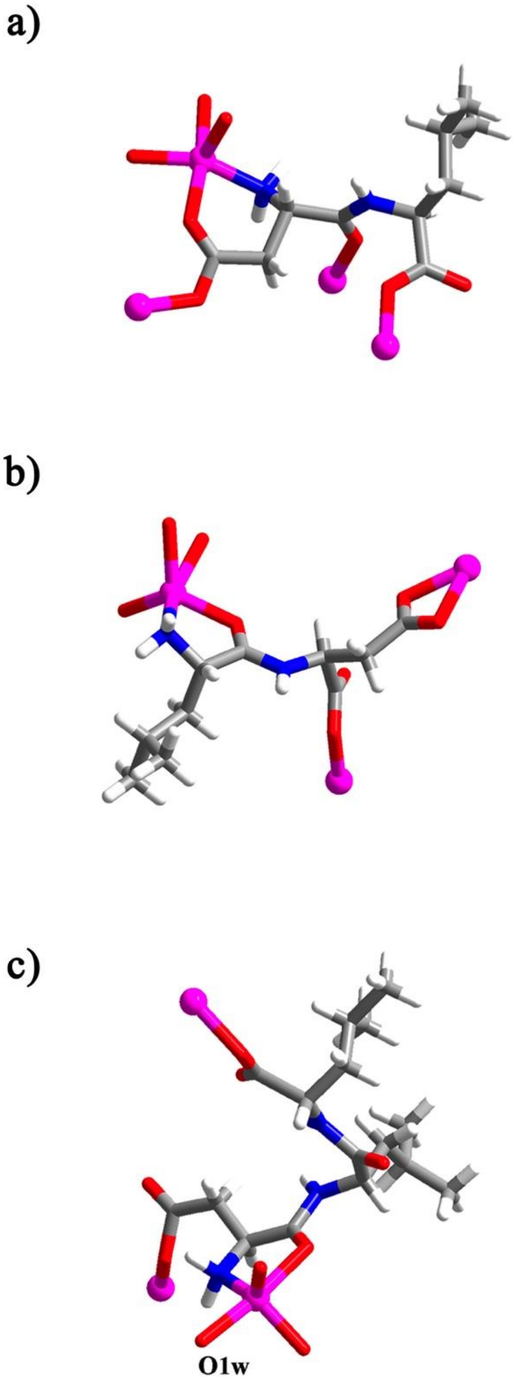

Figure S8. View of the packing of the zig-zag honeycomb layers through H-bond interactions in **2**.

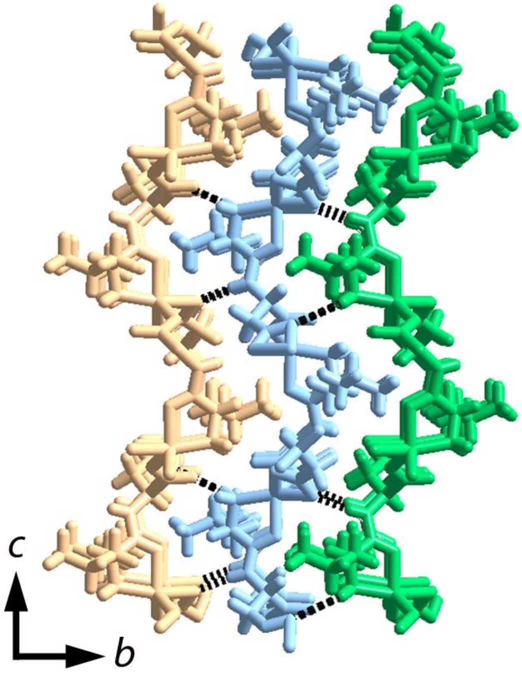

Figure S9. Representation of the –CH atoms of the Leu isobutyl side chains within the Velcro-like Leu motif in **3** and their corresponding distances in Å. The Leu isobutyl chains pointing upwards and downwards are colored in orange and blue, respectively.

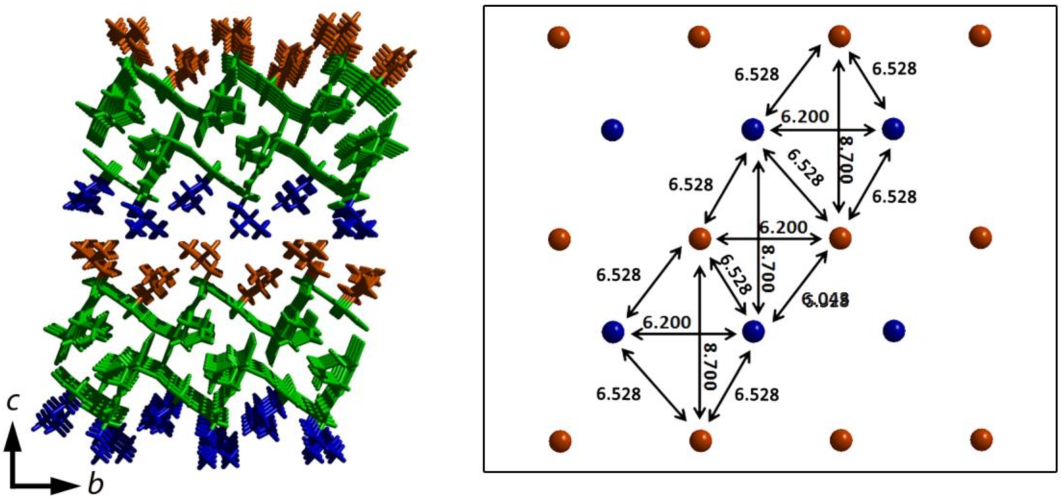

Figure S10. AFM images of pressed pellet disks of **1** (a), **2** (b) and **3** (c).

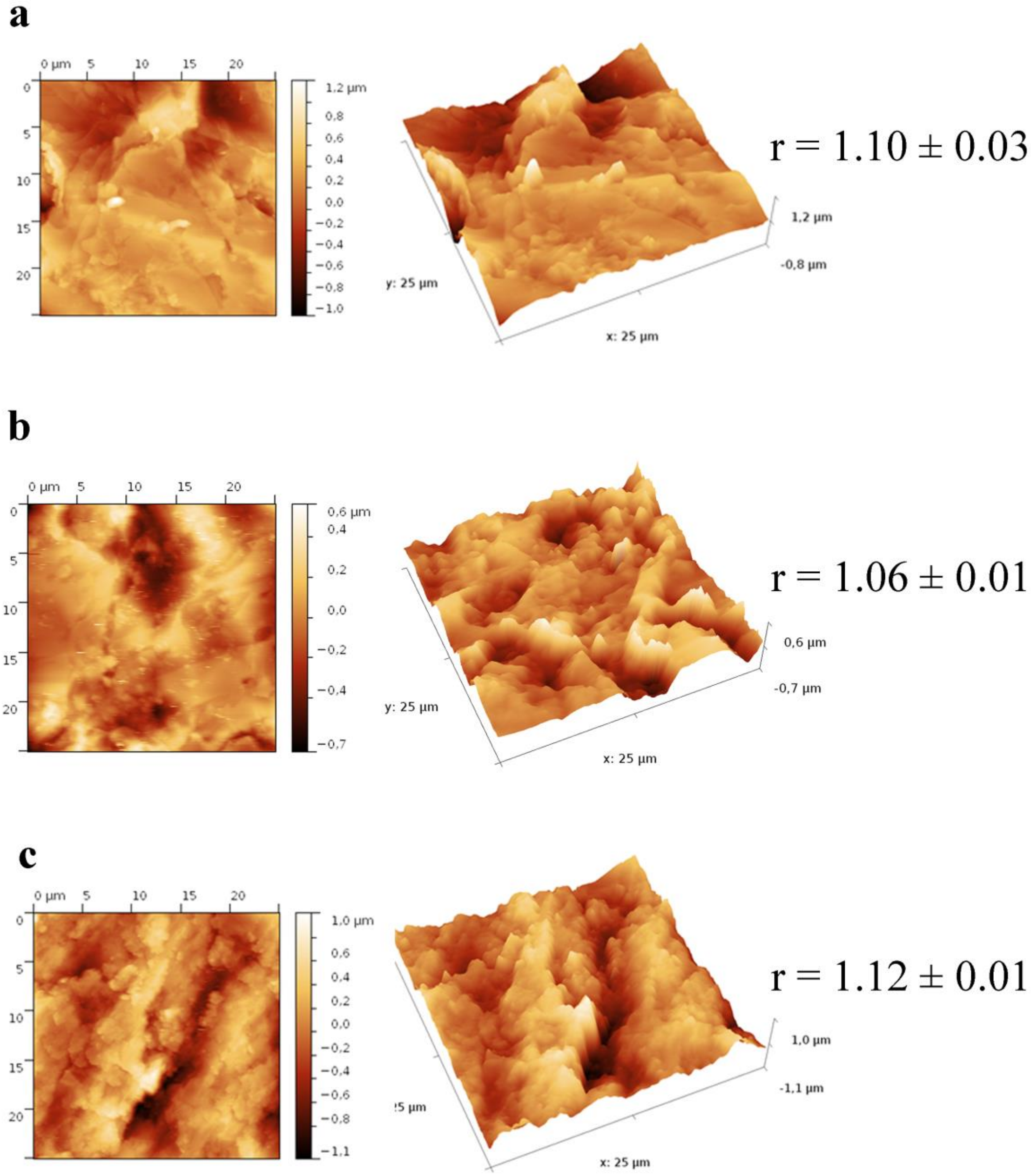

r = 1.10 ± 0.03

r = 1.06 ± 0.01

r = 1.12 ± 0.01

S1.7. References

(1) J. Juanhuix, F. Gil-Ortiz, G. Cuní, C. Colldelram, J. Nicolás, J. Lidón, E. Boter, C. Ruget, S. Ferrer, J. Benach, *J. Synchrotron Rad.* 2014, **21**, 679.

(2) L. Kissel, R. H. Pratt, *Acta Cryst. Sec.A* 1990 **46**, 170

(3) G. M. Sheldrick, Z. Dauter, K. S. Wilson, H. Hope, L. C. Sieker, *Acta Cryst.* 1993, **D49**, 18.

(4) G. M. Sheldrick, *Acta Cryst.* 2015, **C71**, 3.

(5) L. J. Farrugia, *J. Appl. Cryst.* 2012, **45**, 849.